Draft version March 30, 2016
Preprint typeset using LaTeX style emulateapj v. 5/2/11

arXiv:1603.08537v1 [astro-ph.GA] 28 Mar 2016

A TECHNIQUE FOR CONSTRAINING THE DRIVING SCALE OF TURBULENCE AND A MODIFIED CHANDRASEKHAR-FERMI METHOD

Jungyeon Cho, Hyunju Yoo
Department of Astronomy and Space Science, Chungnam National University, Daejeon, Korea; jcho@cnu.ac.kr, hyunju527@gmail.com
Draft version March 30, 2016

ABSTRACT

The Chandrasekhar-Fermi method is a powerful technique for estimating the strength of the mean magnetic field projected on the plane of the sky. In this paper, we present a technique for improving the Chandrasekhar-Fermi method, in which we take into account the averaging effect arising from independent eddies along the line of sight . In the conventional Chandrasekhar-Fermi method, the strength of fluctuating magnetic field divided by $\sqrt{4\pi\bar{\rho}}$, where $\bar{\rho}$ is average density, is assumed to be comparable to the line-of-sight velocity dispersion. This however is not true when the driving scale of turbulence L_f, i.e. the outer scale of turbulence, is smaller than the size of the system along the line of sight L_{los}. In fact, the conventional Chandrasekhar-Fermi method over-estimates the strength of the mean plane-of-the-sky magnetic field by a factor of $\sim\sqrt{L_{los}/L_f}$. We show that the standard deviation of centroid velocities divided by the average line-of-sight velocity dispersion is a good measure of $\sqrt{L_{los}/L_f}$, which enables us to propose a modified Chandrasekhar-Fermi method.

Subject headings: ISM: magnetic fields — magnetohydrodynamics (MHD) — turbulence — techniques: polarimetric

1. INTRODUCTION

Magnetic fields play important roles in many astrophysical environments. However, measuring the strength of them is a very challenging problem. The Chandrasekhar-Fermi method (Chandrasekhar & Fermi 1953; hereinafter the CF method) is a simple and powerful technique that can measure the strength of regular magnetic field perpendicular to the line of sight, i.e. the component of the mean magnetic field projected on the plane of the sky.

The idea of the CF method is simple. Let us consider a fluid filled with Alfvén waves or Alfvénic turbulence. In Alfvénic disturbances, the r.m.s. fluctuation of magnetic field (δb) and the r.m.s. velocity (δv) are related by

$$\frac{\delta b}{\sqrt{4\pi\bar{\rho}}}\sim\delta v \quad \text{or} \quad 1\sim\sqrt{4\pi\bar{\rho}}\frac{\delta v}{\delta b}, \tag{1}$$

where $\bar{\rho}$ is average density. If we multiply both sides by the mean plane-of-the-sky magnetic field $B_{0,sky}$, we obtain

$$B_{0,sky}\sim\sqrt{4\pi\bar{\rho}}\frac{\delta v}{\delta b/B_{0,sky}}. \tag{2}$$

If the velocity fluctuation (δv) and the magnetic field fluctuation (δb) are isotropic, then we may write $\delta v_{los}/\delta b_{\perp,sky}\sim\delta v/\delta b$, where δv_{los} is the line-of-sight velocity dispersion and $\delta b_{\perp,sky}$ is the r.m.s. fluctuation of the plane-of-the-sky magnetic field that is perpendicular to $B_{0,sky}$. Therefore, the equation above becomes

$$B_{0,sky}=\xi\sqrt{4\pi\bar{\rho}}\frac{\delta v_{los}}{\delta b_{\perp,sky}/B_{0,sky}}\sim\xi\sqrt{4\pi\bar{\rho}}\frac{\delta v_{los}}{\delta\phi}, \tag{3}$$

where $\delta\phi$ is the variation of the angle between the plane-of-the-sky magnetic field and the mean plane-of-the-sky magnetic field $\mathbf{B}_{0,sky}$, and we use

$$\delta\phi\sim\tan(\delta\phi)=\delta b_{\perp,sky}/B_{0,sky}. \tag{4}$$

The factor ξ is a correction factor, which is usually taken as $\sim$0.5 (Ostriker et al 2001; Padoan et al. 2001; Heitsch et al. 2001). We can obtain $\delta\phi$ from observations of star-light polarization or polarized far-infrared emission from magnetically aligned dust grains and we can measure δv_{los} from the width of an optically thin molecular emission line (see, for example, Gonatas et al. 1990; Lai et al. 2001; Di Francesco et al. 2001; Crutcher et al. 2004; Girart et al. 2006; Curran & Chrysostomou 2007; Heyer et al 2008; Mao et al. 2008; Tang et al. 2009; Sugitani et al. 2011). Further elaboration of the CF method has been made by many researchers (Zweibel 1990; Myers & Goodman 1991; Zweibel 1996; Ostriker et al. 2001; Heitsch et al. 2001; Padoan et al. 2001; Kudoh & Basu 2003; Wiebe & Watson 2004; Falceta-Gonçalves et al. 2008; Hildebrand et al. 2009; Houde et al 2009).

Reduction of $\delta\phi$ due to averaging effects is of great importance in our paper. Roughly speaking, two main averaging effects exist. First, averaging along the line of sight can reduce $\delta\phi$. That is, if there are more than one independent turbulent eddies along the line of sight, the measured value of $\delta\phi$ will be reduced (see Myers & Goodman 1991; Zweibel 1996; Houde et al 2009). Second, averaging the polarization angle within the telescope beam can also reduce $\delta\phi$ (see Heitsch et al. 2001; Wiebe & Watson 2004; Falceta-Gonçalves et al. 2008; Houde et al. 2009). The averaging effects in general make the step from Equation (2) to Equation (3) inaccurate. In the presence of the averaging effects, the CF method tends to overestimate $B_{0,sky}$.

In this paper, we focus on the averaging effect along the line of sight and propose a simple method to compensate the effect. Using 3-dimensional direct magnetohydrodynamic (MHD) turbulence simulations, we test the proposed technique. In §2, we describe our numerical method and explain in detail how averaging along the line of sight makes the conventional CF method overestimate

$B_{0,sky}$. At the end of §2, we describe our new technique. In §3, we present results of our numerical simulations. In §4, we give discussions and summary.

2. NUMERICAL METHOD AND THEORETICAL CONSIDERATIONS

2.1. *Numerical code*

To obtain turbulence data, we solve the following compressible MHD equations in a periodic box of size 2π using an Essentially Non-Oscillatory scheme (see Cho & Lazarian 2002):

$$\partial\rho/\partial t + \nabla\cdot(\rho\mathbf{v}) = 0, \quad (5)$$

$$\partial\mathbf{v}/\partial t + \mathbf{v}\cdot\nabla\mathbf{v} + \rho^{-1}\nabla(C_s^2\rho) - (\nabla\times\mathbf{B})\times\mathbf{B}/4\pi\rho = \mathbf{f}, \quad (6)$$

$$\partial\mathbf{B}/\partial t - \nabla\times(\mathbf{v}\times\mathbf{B}) = 0, \quad (7)$$

with $\nabla\cdot\mathbf{B}$=0 and an isothermal equation of state P=$C_s^2\rho$, where C_s is the sound speed and ρ is density. Here $\mathbf{v}$ is the velocity, $\mathbf{B}$ is the magnetic field, and $\mathbf{f}$ is the driving force. We use 512^3 grid points. In our simulations, C_s = 0.1, $\bar{\rho}$ = 1, and $B_0/\sqrt{4\pi\bar{\rho}}$ = 1. In all simulations, the r.m.s. velocity v_{rms} is between ∼0.7 and ∼0.8, and the sonic Mach number is $M_s \equiv v_{rms}/C_s \sim 7$. Since the Alfvén speed of the mean field ($V_A = B_0/\sqrt{4\pi\bar{\rho}}$) is 1, the Alfvén Mach number is $M_A \equiv v_{rms}/V_A \sim 0.7$, which means that turbulence considered in this paper is sub-Alfvénic.

2.2. *Forcing*

In this work, we drive turbulence in Fourier space and consider only solenoidal ($\nabla\cdot\mathbf{f} = 0$) forcing. We use ∼100 forcing components isotropically distributed in the range $k_f/1.3 \lesssim k \lesssim 1.3k_f$, where k is the wavenumber and k_f varies from simulation to simulation (see Table 1). Therefore, the peak of energy injection occurs at k $\sim k_f$. More detailed descriptions on forcing can be found in Yoo & Cho (2014).

2.3. *Theoretical Considerations: The Effects of Averaging along a Line of Sight*

Our main concern is to investigate the effect of the driving scale on the CF method. For this purpose, we change the driving scale by changing the driving wavenumber k_f.

If the driving scale is L_f, then there are $\sim L_{los}/L_f$ ($\equiv N$) large-scale eddies (i.e. largest energy-containing eddies) along a line of sight, where L_{los} is the size of the system along the line of sight (see Figure 1(a))[1]. In this case, what will be the strength of observed magnetic field projected on the plane of the sky? If we take a coordinate system as shown in Figure 1(a), the plane of the sky is parallel to the xy-plane. Let us consider the x and y-components of magnetic field separately. Here x and y-directions are parallel and perpendicular to the mean plane-of-the-sky magnetic field, respectively. We can write

$$B_{x,obs} \propto \int_0^{L_{los}} B_x dz \sim B_{0,sky}L_{los}, \quad (8)$$

[1] In our simulations, $L_{los} = 2\pi$ and $L_f \sim 2\pi/k_f$. Therefore, if the driving wavenumber is k_f, then the number of independent eddies along a line of sight is $N = L_{los}/L_f \sim k_f$.

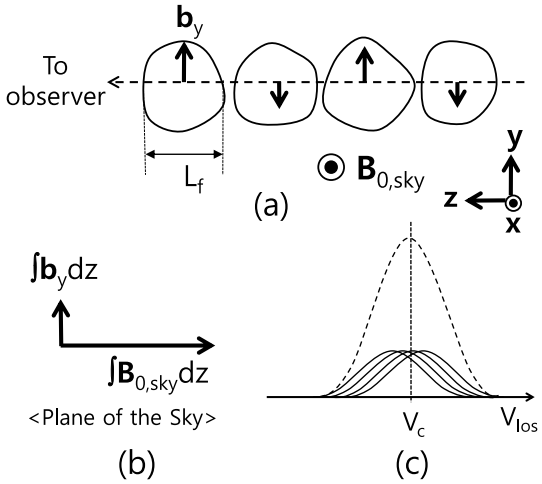

FIG. 1.— Effects of averaging along the line of sight. (a) If the driving scale of turbulence is L_f in a strongly magnetized medium, we have $\sim L_{los}/L_f$ ($\equiv N$) independent eddies along the line of sight. Here L_{los} is the size of the system along the line of sight. The field $\mathbf{B}_{0,sky}$ denotes the mean plane-of-the-sky magnetic field. The y-component of magnetic field in each eddy is likely to be random. (b) The x-component of observed magnetic field is equal to $\int B_{0,sky}dz \sim B_{0,sky}L_{los}$, if we ignore contribution from random magnetic field along x-direction. The y-component of observed magnetic field is $\sim \int b_y dz \sim (b_y L_f)\sqrt{L_{los}/L_f}$. (c) The solid lines denote line profiles from individual eddies and the dashed line stands for observed line profile. The mean velocity of each eddy can be different from each other. The observed centroid velocity V_c is approximately the average of the mean velocities of individual eddies along the line of sight.

$$b_{y,obs} \propto \int_0^{L_{los}} b_y dz \sim b_y L_f \sqrt{\frac{L_{los}}{L_f}} = b_y\sqrt{L_f L_{los}}, \quad (9)$$

where we ignore the contribution of random magnetic field in the integration of B_x ($\equiv B_{0,sky} + b_x$) and assume that each large-scale eddy contributes randomly in the integration of b_y (see Figure 1(b))[2]. Therefore, the variation of the angle between the magnetic field projected on the plane of the sky and the mean plane-of-the-sky magnetic field is given by

$$\delta\phi \sim \tan(\delta\phi) \sim \frac{b_{y,obs}}{B_{x,obs}} \sim \frac{b_y}{B_0}\sqrt{L_f/L_{los}}, \quad (10)$$

which is $(L_{los}/L_f)^{1/2}$ times smaller than the conventional estimate of $\delta\phi$ (see Equation (4)).

Indeed, our simulations confirm that, the larger the number of independent eddies along the line of sight L_{los}/L_f is, the smaller the variation $\delta\phi$ is. Using our MHD turbulence data (see Table 1) and numerical method in Fiege & Pudritz (2000; see also Heitsch et al. 2001), we obtain synthetic polarization maps arising from magnetically-aligned dust grains at a far-infrared/sub-mm wavelength. We show the maps for runs with differ-

[2] The length-scale L_f in Equation (9) should be the coherence scale of magnetic field (see Cho & Ryu 2009). In this paper, we assume that the coherence scale coincides with the driving scale of turbulence, which is a very good approximation for trans-Alfvénic or sub-Alfvénic turbulence, i.e. turbulence in which the r.m.s. velocity is similar to or less than the Alfvén speed of the mean magnetic field. In sub-Alfvénic turbulence, the magnetic energy spectrum peaks at the driving scale and, therefore, the coherence scale of magnetic field should be very close to the driving scale of turbulence.

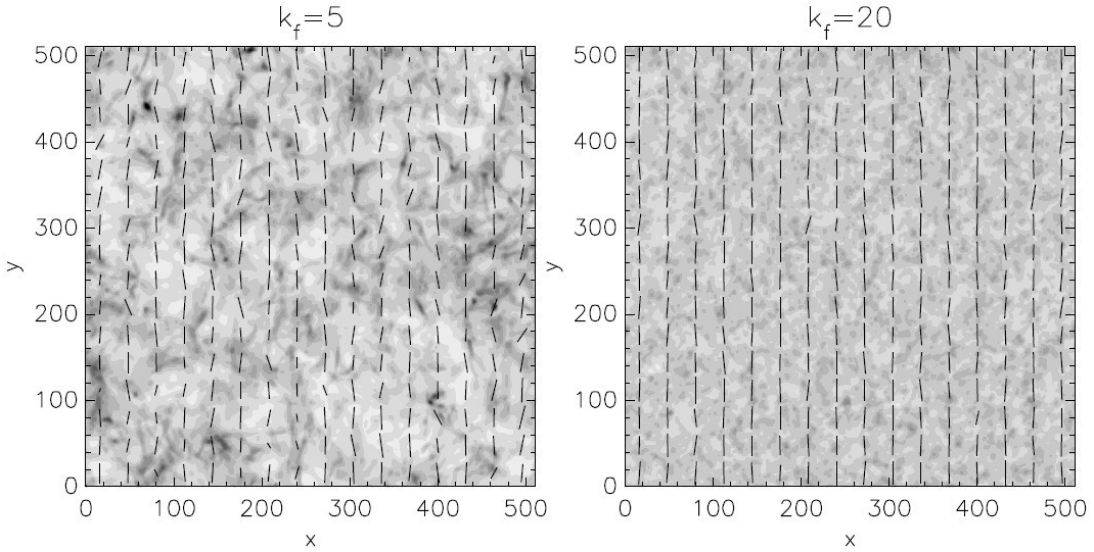

FIG. 2.— Reduction of variation in polarization angle $\delta\phi$ due to averaging effect along the line of sight. The driving wavenumbers, hence the number of independent eddies along a line of sight, are different in the left and right panels. *Left:* The driving wavenumber is ~ 5 and therefore there are approximately 5 independent eddies along a line of sight. *Right:* The driving wavenumber is ~ 20 and there are approximately 20 independent eddies along a line of sight. Variation in polarization angle is smaller in the right panel due to larger number of independent eddies along the line of sight. The contours represent intensity of FIR/sub-mm emission from magnetically aligned dust. The polarization maps are taken after saturation of turbulence. The left and the right panels are from Runs KF5 and KF20, respectively. The projections are done along a line of sight perpendicular to the mean field $\mathbf{B}_0$.

ent driving scales in Figure 2. The coordinate system we adopted is similar to the one in Figure 1: we assumed the mean magnetic field is along the x-axis and the observer's line of sight is along the z-axis. Since the mean magnetic field is along the x-axis, the direction of polarization is mainly along the y-axis. In the left panel, the driving scale is $\sim$5 times smaller than the size of the computational box (Run KF5) and in the right panel the driving scale is $\sim$20 times smaller than the size of the computational box (Run KF20). We can clearly see that the variation of polarization angle in the left panel ($N\sim5$) is larger than that in the right panel ($N\sim20$), which illustrates that the dispersion in polarization angle is indeed a function of N ($\sim L_{los}/L_f$) as discussed in the previous paragraph. The standard deviations of polarization angle in the left and right panels are $\sim 9.1^\circ$ and $\sim 3.5^\circ$, respectively. Note that the 3-dimensional magnetic fluctuations in both runs are similar (see the left panel of Figure 3).

2.4. *Observational Estimation of* (L_f/L_{los})

From the discussion in the previous subsection, it is clear that the conventional CF method overestimates the strength of the mean plane-of-the-sky magnetic field by a factor of $\sqrt{L_{los}/L_f}$. Therefore it is necessary to know $\sqrt{L_{los}/L_f}$ to obtain a correct estimate of $B_{0,sky}$.

We propose that the standard deviation of centroid velocities δV_c normalized by the average line-of-sight velocity dispersion δv_{los} is a good measure of $\sqrt{L_{los}/L_f}$ ($\approx\sqrt{N}$):

$$\frac{\delta V_c}{\delta v_{los}} \propto \frac{1}{\sqrt{N}}, \tag{11}$$

where

$$V_c = \int v_{los} I(v_{los}) dv_{los} \Big/ \int I(v_{los}) dv_{los} \tag{12}$$

and $I(v_{los})$ is the observed line profile for the line of sight.

Centroid velocity V_c is a kind of average velocity. If we have several independent eddies along the line of sight, then each eddy has its own mean velocity. Then, roughly speaking, the observed centroid velocity for the line of sight is average of the mean velocities of individual eddies along the line of sight. Note that the mean velocities of independent eddies are likely to be random. Therefore, if we obtain centroid velocities for many different lines of sight and calculate standard deviation of them, then the standard deviation should be proportional to $\sim 1/\sqrt{N}$, where N is the number of independent eddies along a line of sight. In Figure 1(a) we draw 4 independent eddies along the line of sight and in Figure 1(c), we plot velocity profiles (or emission line profiles) from 4 independent eddies in solid lines and the observed line profile in dashed line. Then, the observed centroid velocity V_c is approximately the average of the mean velocities of 4 eddies. If we have more eddies along the line of sight, the variation in velocity centroids normalized by the average width of an optically thin emission line will become smaller.

3. RESULTS

The left panel of Figure 3 shows the time evolution of $(\delta v)^2$ and $B^2/(4\pi\bar{\rho})$, where $B^2 = B_0^2 + (\delta b)^2$. At t=0, $(\delta v)^2 \approx 0$ and only the uniform magnetic field of unit Alfvén speed (i.e. $B_0/\sqrt{4\pi\bar{\rho}} = 1$) exists. Due to driving, $(\delta v)^2$ and $B^2/(4\pi\bar{\rho})$ grows initially. After $t \sim 2(L_f/\delta v)$, turbulence seems to show saturation in all simulations.

The right panel of Figure 3 shows the time evolution of

$$\sqrt{k_f}\delta V_c/\delta v_{los} \quad (\approx \sqrt{N}\delta V_c/\delta v_{los}), \tag{13}$$

where δv_{los} is the average line-of-sight velocity dispersion. The standard deviation of centroid velocities δV_c and the average of line-of-sight velocity dispersion δv_{los} are calculated over 512^2 lines of sight perpendicular

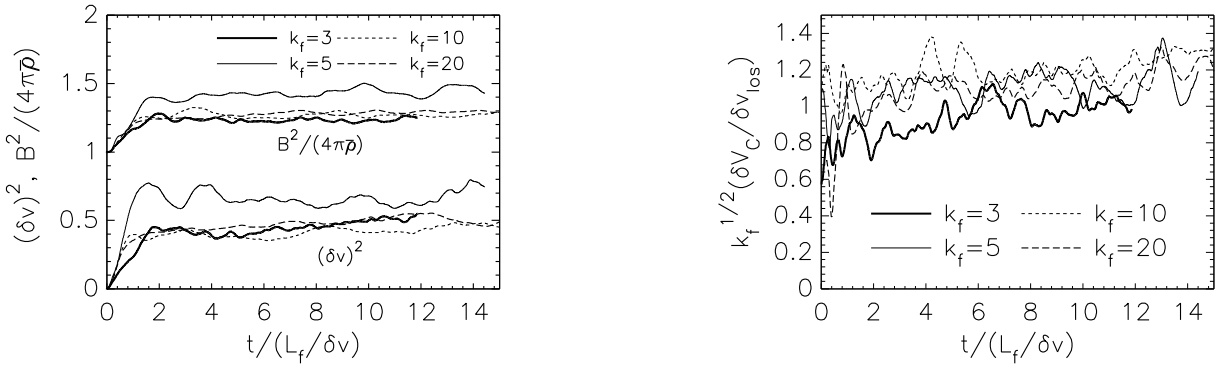

FIG. 3.— *Left:* Time evolution of $(\delta v)^2$ and $B^2/(4\pi\bar{\rho})$. *Right:* Time evolution of $\sqrt{k_f}$ times the standard deviation of velocity centroids δV_c divided by the average line-of-sight velocity dispersion δv_{los}, where k_f is the driving wavenumber (see Equation (13) for details). In both plots, the x-axes denote time normalized by $L_f/\delta v$, where L_f is the driving scale of turbulence and δv is the r.m.s. velocity.

to the mean field $\mathbf{B_0}$. The figure confirms that the quantity $\delta V_c/\delta v_{los}$ is indeed proportional to $1/\sqrt{k_f}$ ($\approx \sqrt{L_f/L_{los}}$), as we proposed in Section 2.4 (see Equation (11)).

The left panel of Figure 4 shows our main result. Since the conventional CF method tends to overestimate $B_{0,sky}$ by a factor of $\sqrt{L_{los}/L_f}$ and $\delta V_c/\delta v_{los} \propto \sqrt{L_f/L_{los}}$ we can write

$$B_{0,sky} = \xi' \sqrt{4\pi\bar{\rho}} \frac{\delta V_c}{\delta \phi}, \tag{14}$$

where ξ' is a constant of order unity that can be determined by numerical simulations. In the left panel of Figure 4 we plot estimates of $B_{0,sky}/\sqrt{4\pi\bar{\rho}}$ from this modified CF method:

$$\frac{\delta V_c}{\delta \phi}. \tag{15}$$

In the panel, we can see that the estimates are fluctuating between ∼1.0 and ∼1.5. Therefore, since $B_{0,sky}/\sqrt{4\pi\bar{\rho}} = 1$ in our simulations, the constant ξ' in Equation (14) is between ∼0.7 and ∼1.

The right panel of Figure 4 shows estimates of $B_{0,sky}/\sqrt{4\pi\bar{\rho}}$ from the conventional CF method:

$$\frac{\delta v_{los}}{\delta \phi}. \tag{16}$$

We can see that the conventional CF method indeed overestimates $B_{0,sky}$ when the number of independent eddies along the line of sight ($\sim k_f$ in our simulations) is large. Note, however, that the conventional CF method seems to work fine for small N's.

4. DISCUSSIONS AND SUMMARY

In this paper, we have considered the effects of driving scale on the estimates of the mean plane-of-the-sky magnetic field $B_{0,sky}$ from the Chandrasekhar-Fermi (CF) method. The method we propose in Equation (14) with $0.7 \lesssim \xi' \lesssim 1.0$ does not require new observations. That is, the method is readily applicable for present observational data. Apart from numerical constants, the only difference between our method and the conventional CF method is that our method requires the standard deviation of velocity centroids δV_c, while the conventional method requires average width of the emission line profiles δv_{los}. The standard deviation of velocity centroids δV_c can be easily obtained from existing optically-thin emission line profiles. If such emission line profiles ($I(v_{los})$'s) are available for n_{obs} lines of sight, then we need the following two steps to obtain δV_c:

1. We calculate the centroid velocity V_c (see Equation (12)) for each line of sight. Let $V_{c,i}$ be the centroid velocity for line of sight i:

$$V_{c,i} = \int v_{los} I_i(v_{los}) dv_{los} \Big/ \int I_i(v_{los}) dv_{los}, \tag{17}$$

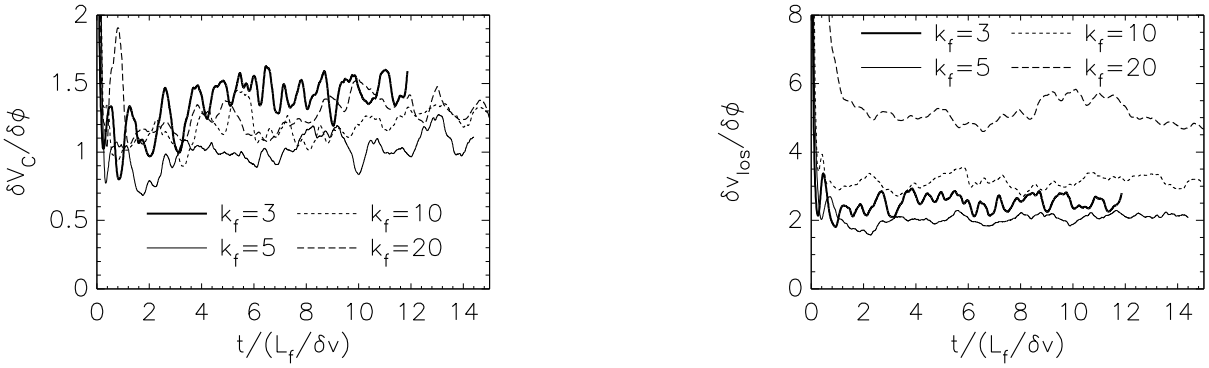

FIG. 4.— Estimates of $B_{0,sky}/\sqrt{4\pi\bar{\rho}}$. *Left:* Results from our modified CF method (see Equation (15)). *Right:* Results from the conventional CF method (see Equation (16)). Note that, in all our simulations, the line of sight is perpendicular to the mean field $\mathbf{B}_0$ and $B_{0,sky}/\sqrt{4\pi\bar{\rho}}$=1. The conventional CF method overestimates $B_{0,sky}$ when there are many independent eddies along the line of sight.

where $I_i(v_{los})$ is the optically-thin emission line profile for the line of sight.

2. We calculate δV_c from the formula

$$\delta V_c^2 \equiv \frac{1}{n_{obs}} \sum_{i=1}^{n_{obs}} V_{c,i}^2 - \left(\frac{1}{n_{obs}} \sum_{i=1}^{n_{obs}} V_{c,i} \right)^2 . \qquad (18)$$

The CF method is useful for obtaining strengths of the plane-of-the-sky magnetic fields in molecular clouds. Since observations suggest existence of supersonic motions and strong magnetic fields in molecular clouds, we have considered only supersonic ($M_s \sim 7$) and marginally sub-Alfvénic ($M_A \lesssim 1$) MHD turbulence in this paper. It is possible that the constant ξ' in Equation (14) depends on the the sonic Mach number M_s. But, we expect that the dependence is weak because the sonic Mach number does not play an important role in our discussion in Section 2.4. Nevertheless, more parameter study is needed to determine the dependence of ξ' on M_s. Another limitation of our current work is that we have considered only the case that the mean magnetic field is perpendicular to the line of sight, which means that the inclination angle (with respect to the plane of the sky) of the mean magnetic field is zero. In principle, our method, as well as the conventional CF method, should work for an arbitrary inclination angle, unless the inclination angle is very close to 90° (see discussions in Ostriker et al. 2001; Heitsch et al. 2001; Falceta-Gonçalves et al. 2008). We will address these issues elsewhere.

In this paper we have demonstrated that the conventional CF method indeed over-estimates the mean plane-of-the-sky magnetic field $B_{0,sky}$ by a factor of $\sqrt{N}$, where N is the number of independent eddies along the line of sight. We have found that the standard deviation of centroid velocities divided by the average line-of-sight velocity dispersion ($\delta V_c/\delta v_{los}$) is proportional to $1/\sqrt{N}$ (Equation (11) and the right panel of Figure 3). Therefore Equation (14) with $\xi' = 0.7 \sim 1$ provides a better estimate for $B_{0,sky}$.

This work is supported by the National R & D Program through the National Research Foundation of Korea, funded by the Ministry of Education (NRF-2013R1A1A2064475). We thank Woojin Kwon, Ellen Zweibel and Alex Lazarian for useful discussions. We also thank the hospitality of the Astronomy Department at the University of Wisconsin - Madison during the final stage of writing.

REFERENCES

Chandrasekhar, S., & Fermi, E. 1953, ApJ, 118, 113

Cho, J., & Lazarian, A. 2002, Physical Review Letters, 88, 245001

TABLE 1
Simulations.

Run	Resolution	M_s [a]	$B_0/\sqrt{4\pi\bar{\rho}}$ [b]	k_f [c]	L_{los}/L_f [d]
KF3	512^3	∼7	1	3	~ 3
KF5	512^3	∼8	1	5	~ 5
KF10	512^3	∼7	1	10	~ 10
KF20	512^3	∼7	1	20	~ 20

[a] Sonic Mach number.
[b] Alfvén speed of mean magnetic field.
[c] Driving wavenumber.
[d] L_{los} is the system size and L_f is the driving scale. In our simulations, L_{los}=2π and $L_f \sim 2\pi/k_f$. Therefore, we have $N = L_{los}/L_f \sim k_f$.

Cho, J., & Ryu, D. 2009, ApJ, 705, L90
Crutcher, R. M., Nutter, D. J., Ward-Thompson, D., & Kirk, J. M. 2004, ApJ, 600, 279
Curran, R. L., & Chrysostomou, A. 2007, MNRAS, 382, 699
Di Francesco, J., Myers, P. C., Wilner, D. J., Ohashi, N., & Mardones, D. 2001, ApJ, 562, 770
Falceta-Gonçalves, D., Lazarian, A., & Kowal, G. 2008, ApJ, 679, 537
Fiege, J. D., & Pudritz, R. E. 2000, ApJ, 544, 830
Girart, J. M., Rao, R., & Marrone, D. P. 2006, Science, 313, 812
Gonatas, D. P., Engargiola, G. A., Hildebrand, R. H., et al. 1990, ApJ, 357, 132
Heitsch, F., Zweibel, E. G., Mac Low, M.-M., Li, P., & Norman, M. L. 2001, ApJ, 561, 800
Heyer, M., Gong, H., Ostriker, E., & Brunt, C. 2008, ApJ, 680, 420
Hildebrand, R. H., Kirby, L., Dotson, J. L., Houde, M., & Vaillancourt, J. E. 2009, ApJ, 696, 567
Houde, M., Vaillancourt, J. E., Hildebrand, R. H., Chitsazzadeh, S., & Kirby, L. 2009, ApJ, 706, 1504
Kudoh, T., & Basu, S. 2003, ApJ, 595, 842
Lai, S.-P., Crutcher, R. M., Girart, J. M., & Rao, R. 2001, ApJ, 561, 864
Mao, S. A., Gaensler, B. M., Stanimirović, S., et al. 2008, ApJ, 688, 1029
Myers, P. C., & Goodman, A. A. 1991, ApJ, 373, 509
Ostriker, E. C., Stone, J. M., & Gammie, C. F. 2001, ApJ, 546, 980
Padoan, P., Goodman, A., Draine, B. T., et al. 2001, ApJ, 559, 1005
Sugitani, K., Nakamura, F., Watanabe, M., et al. 2011, ApJ, 734, 63
Tang, Y.-W., Ho, P. T. P., Girart, J. M., et al. 2009, ApJ, 695, 1399
Wiebe, D. S., & Watson, W. D. 2004, ApJ, 615, 300
Yoo, H., & Cho, J. 2014, ApJ, 780, 99
Zweibel, E. G. 1990, ApJ, 362, 545
Zweibel, E. G. 1996, Polarimetry of the Interstellar Medium, 97, 486